nearly complete pyrolysis of Me_3Ga to MeGa at temperatures above 600 °C and pressures similar to those used in this study.[18]

The above analysis of growth data for four different organometallic arsenic sources combined with either Me_3Ga or Et_3Ga shows that a model based on reversible adduct formation between arsenic and gallium source compounds and subsequent gas-phase reactions depleting film precursors in competition with the growth process is consistent with the experimental observations. However, adduct formation has not been reported in MOCVD growth of GaAs from t-$BuAs_2$ and Me_3Ga at atmospheric pressures.[3,4,8,14] Fundamental organometallic studies[30,32] as well as the recent emphasis on the use of adducts as source materials[23-28] demonstrate that donor–acceptor complexes form between arsenic and gallium compounds used in the present study. The question is whether the adduct is sufficiently stable to survive in the entrance zone and undergo internal rearrangement or whether it falls apart into the original alkyls. The microbalance reactor, used in the present study, has a relatively small heated volume in contrast to standard MOCVD systems, which also have long entrance zones. Furthermore, the microbalance system operates at low pressure, so that the growth is controlled by chemical kinetics, while mass-transfer influences the growth in atmospheric MOCVD reactors.[1] This difference is reflected in the large growth rates, ~ 20–30 μm/h, measured in the microbalance system in contrast to 1–5 μm/h achieved in conventional systems. The variation in growth rate with flow rates, which reveals the presence of adduct-related parasitic reactions in this work, is confined to growth rates higher than those typically measured in standard systems. Thus, it is possible that transport effects mask the adduct-related deposition phenomena in conventional reactors. Furthermore, because of the time-consuming task of obtaining growth rate data in standard systems, relatively few growth rate data[2,4,8] have been reported compared to the large number of data points generated with the microbalance reactor. Perhaps an extensive study of growth rate variations with flow rates, feed combinations, source compounds, and growth temperatures would reveal a mechanism similar to the model proposed here. Ultimately, the question about the actual growth mechanism will have to be resolved through careful spectroscopic identification of possible adduct intermediates and related decomposition reaction products.

Acknowledgment. This work was supported financially by the National Science Foundation (CBT-8351249, DMR 8704355) and Air Products and Chemicals. We are grateful to S. Brandon and M. Hoveland for help with the mass spectrometer and characterization studies. We also thank T. F. Kuech for help with photoluminescence and American Cyanamid for assistance with the t-$BuAsH_2$.

Registry No. GaAs, 1303-00-0; Et_3Ga, 1115-99-7; Me_3Ga, 1445-79-0; Me_3As, 617-75-4; Et_3As, 617-75-4; t-$BuAsH_2$, 4262-43-5; $PhAsH_2$, 822-65-1.

Surface Characterization of Radio Frequency Water Plasma Treated and Annealed Polycrystalline Tin Oxide Thin Films

Michael J. Tarlov† and John F. Evans*

Department of Chemistry, University of Minnesota, Minneapolis, Minnesota 55455

Received May 11, 1989

Angle-resolved X-ray photoelectron spectroscopy (AR-XPS) and electron energy loss spectroscopy (EELS) have been used to examine the consequences of the interaction of radio frequency water plasmas with polycrystalline tin oxide surfaces. Results from AR-XPS and EELS indicate that an extensive surface hydroxylation or "gel" layer (>10 Å) does not form on the tin oxide surface from exposure to atmosphere and/or water plasma treatment. Surface hydroxyl coverages determined by AR-XPS are a factor of 3 lower than those calculated from crystallographic models. Annealing of water plasma treated tin oxide films in ultrahigh vacuum results in the desorption of water, dehydroxylation of the surface, and creation of oxygen vacancies. AR-XPS data indicate a uniform concentration of oxygen vacancies over a sampling depth of approximately 15 Å. Water plasma treatment of oxygen-deficient tin oxide surfaces created by annealing in ultrahigh vacuum eliminates oxygen vacancies and restores Sn^{4+} valency in the surface region.

Introduction

Tin oxide (SnO_2) is an n-type, wide-bandgap (3.6 eV), metal oxide semiconductor.[1-3] When doped with antimony or fluorine, it becomes a quasimetallic conductor while retaining optical transparency in the visible region and a high reflectivity for infrared radiation. Many methods exist for the deposition of highly conductive, transparent, tin oxide films. This has allowed them to be used as transparent heating elements, heat refleting shields, and transparent electrical contacts.[4-6] In addition, tin oxide has been widely used as a gas-sensing element for the detection of H_2, CO, hydrocarbons, and alcohols.[7,8]

†Permanent Address: Chemical Process Metrology Division, National Institute of Standards and Technology, Gaithersburg, MD 20899.

(1) Jarzebski, Z. M.; Marton, J. P. *J. Electrochem. Soc.* **1976**, *123*, 199c.
(2) Jarzebski, Z. M.; Marton, J. P. *J. Electrochem. Soc.* **1976**, *123*, 299c.
(3) Jarzebski, Z. M.; Marton, J. P. *J. Electrochem. Soc.* **1976**, *123*, 333c.
(4) DeWaal, H.; Simonis, F. *Thin Solid Films* **1981**, *77*, 253.
(5) Frank, G.; Kauer, H.; Köstlin, L.; Kauer, E. *Thin Solid Films* **1981**, *77*, 107.
(6) Manifacier, J. C. *Thin Solid Films* **1982**, *100*, 297.
(7) McAleer, J. F.; Mosely, P. T.; Norris, J. O. W.; Williams, D. E. *J. Chem. Soc., Faraday Trans. 1* **1988**, *83*, 1323.
(8) McAleer, J. F.; Mosely, P. T.; Norris, J. O. W.; Williams, D. E.; Tofield, B. C. *J. Chem. Soc., Faraday Trans. 1* **1988**, *84*, 441.

0897-4756/90/2802-0049$02.50/0

Tin oxide has also been used extensively in electrochemical studies, where its high conductivity and transparency make it suitable as an optically transparent working electrode for spectroelectrochemical studies.[9] The tin oxide/aqueous electrolyte interface has been investigated as a model metal oxide electrode system by using impedance methods, and in all cases anomalies have been observed in its electrochemical behavior.[10-13] This nonideal electrochemical behavior has usually been interpreted in terms of a surface-related phenomenon, the most common being the hydroxylation and/or hydration of the tin oxide surface region. Bressel and Gerischer have reported that a 25-Å-thick mixed oxide/hydroxide surface layer forms on tin oxide films immersed in aqueous electrolytes based on Auger and IR reflection data.[13] Armstrong and Shepard associated frequency-dependent capacitance results with a surface-state capacitance arising from mobile ionic species in a hydrated, "gellike", surface layer.[12] Using X-ray photoelectron spectroscopy in conjunction with ion sputtering, they estimated the hydrated surface layer thickness to be at least 100–200 Å, although detailed data were not presented. It was recently reported that hydration of polycrystalline tin oxide films from exposure to atmospheric humidity for several months occurs to depths of at least 30 Å.[14]

The model of a porous "gel layer" was first developed to account for the experimentally determined high surface charge and modest diffuse layer potential of various colloidal metal oxide systems in aqueous solutions.[15] In this model hydronium and hydroxyl ions are capable of penetrating the oxide surface and reacting with amphoteric hydroxyl groups to produce charged sites in a three-dimensional matrix. In addition, ion-exchange reactions in this layer can occur from penetration of counterions to maintain electroneutrality. In a previous study, various thin-film analytical techniques were used to characterize sputter-deposited tin oxide films before and after immersion in aqueous solutions to determine the extent of film hydration and ion-exchange activity.[16] The results supported a model in which the tin oxide film is comprised of microcrystalline, colloidlike particles or grains (200–300 Å) with ion-exchange sites located on hydroxylated grain surfaces.

In this paper, results from a detailed investigation of the surface composition and electronic structure of hydroxylated polycrystalline tin oxide films are presented and discussed. It is demonstrated that radio frequency (rf) water plasma treatment of tin oxide films is an excellent method for preparing "clean", model, hydroxylated surfaces. These model, hydroxylated surfaces were examined by angle-resolved X-ray photoelectron spectroscopy (AR-XPS) and electron energy loss spectroscopy (EELS). Line-shape analysis of the O(1s) photoelectron line at different emission angles and the description of these data by theoretical working curves were used to determine the hydroxylated layer stoichiometry and thickness. Valence band XPS (VB-XPS) and EELS were used to examine the surface electronic structure and yielded information that was complementary to that from core-level XPS.

One difficulty in studying tin oxide surfaces is that the tin core-level photoelectron lines exhibit no significant binding energy shift between the stannous (SnO) and stannic (SnO_2) oxides. It has been shown, however, that both VB-XPS[17] and EELS[18] can qualitatively distinguish between SnO and SnO_2. In addition, it has been reported that VB-XPS and EELS can detect changes in the tin oxide lower valence band density of states that are indicative of hydrated subsurface layers.[14]

Another difficulty in examining tin oxide surfaces (and metal oxide surfaces in general) is reproducibly preparing clean surfaces of known stoichiometry. Because tin oxide surfaces, hydroxylated by exposure to atmospheric humidity, were of special interest in this study, it was necessary to develop surface-cleaning methods capable of removing surface carbon contaminaton while not altering the hydrated surface layer. It was found in the course of this work that oxygen-containing carbon contamination (originating from exposure to atmosphere) could contribute significantly to the O(1s) line shape. Thus, the removal of surface carbon contamination was imperative to perform a detailed line-shape analysis of the O(1s). Ion bombardment of a metal oxide commonly results in the preferential removal of oxygen with concomitant reduction of the surface and, thus, was unsuitable. Likewise, high-temperature annealing can cause the desorption of surface-bound water and decomposition of the oxide.

In this work, rf water plasmas were used as an alternative method for cleaning tin oxide surfaces. Previous studies in this laboratory demonstrated that low-power rf water discharges could effectively remove carbon contamination from metal oxide surfaces while largely preserving the hydrated surface structure.[19] The detailed mechanism of surface cleaning by exposure to low-power water plasmas is not fully understood but clearly involves oxidation of adsorbed carbonaceous material to less tightly bound surface species. Furthermore, desorption is assisted by low-energy ion bombardment. Damage effects from ion bombardment, such as preferential sputtering and lattice disordering, are largely avoided by operating the plasma at relatively low powers. This is substantiated below by EELS spectra acquired from water plasma treated tin oxide films that are characteristic of a well-crystallized surface.

This paper is presented as follows. First, data from AR-XPS and EELS of water plasma treated tin oxide films previously exposed to atmosphere are presented and discussed. The extent of hydroxylation is estimated from modeling of the curve-fitted O(1s) AR-XPS data. These results are discussed in relation to crystallographic models for hydroxylation of the SnO_2 surface and to hydroxyl surface densities for SnO_2 reported in the literature. VB-XPS and EELS spectra indicate that water plasma treatment of the tin oxide films produce a fully oxidized, Sn^{4+}-like surface and that the surface electronic structure is similar to that of the bulk. Second, the thermal stability of the hydrated layer is examined. XPS and EELS results indicate that in vacuo annealing of the water plasma treated tin oxide film leads to the loss of adsorbed water, dehydroxylation of the surface, and creation of oxygen vacancies at and below the surface. Third, we show that

(9) Winograd, N.; Kuwana, T. *Electroanalytical Chemistry*; Bard, A. J., Ed.; Dekker: New York, 1974.
(10) Elliot, D.; Zellmer, D. L.; Laitinen, H. A. *J. Electrochem. Soc.* **1970**, *134*, 66.
(11) McCann, J. F.; Badwal, S. P. S.; Pezy, J. *J. Electroanal. Chem.* **1981**, *118*, 115.
(12) Armstrong, N. R.; Shepard, Jr., V. R. *J. Phys. Chem.* **1981**, *85*, 2965.
(13) Bressel, B.; Gerischer, H. *Ber. Bunsen-Ges Phys. Chem.* **1983**, *87*, 398.
(14) Cox, D. F.; Hoflund, G. B.; Laitinen, H. A. *Appl. Surf. Sci.* **1984**, *20*, 30. Cox, D. F.; Hoflund, G. B.; Hocking, W. H. *Appl. Surf. Sci.* **1986**, *26*, 239. Hoflund, G. B.; Grogan, A. L., Jr.; Asbury, D. A.; Schryer, D. R. *Thin Solid Films* **1989**, *169*, 69.
(15) Lyklema, J. *J. Electroanal. Chem.* **1968**, *18*, 341.
(16) Tarlov, M. J.; Evans, J. F. *J. Vac. Sci. Technol.* **1987**, *A5*(4), 941.
(17) Lau, C.; Wertheim, G. K. *J. Vac. Sci. Technol.* **1978**, *15*, 622.
(18) Powell, R. A. *Appl. Surf. Sci.* **1979**, *2*, 397.
(19) Newman, J. G. M.S. Thesis, University of Minnesota, 1984.

water plasma treatment of the in vacuo annealed tin oxide surface regenerates the original water plasma treated surface.

Experimental Section

Polycrystalline tin oxide films prepared by rf sputter deposition and by a spray hydrolysis method were used in this study. All sputter-deposited tin oxide films were prepared by reactive sputtering of a 99.99% tin target in a 50:50 argon:oxygen atmosphere at a total pressure of 10–12 mTorr. At an applied rf power of 500 W (which developed 1700–1800 V on the target) the deposition rate was approximately 100 Å/min. A detailed description of the sputter-deposition system and parameters is given elsewhere.[20] Single-crystal phosphorous-doped, n-type silicon(100) was used as a substrate material and was cleaned by using standard methods. For certain experiments a 200–300-Å SiO_2 layer was grown thermally on the silicon wafer and was used as the substrate. No differences were observed between tin oxide films deposited on SiO_2 or Si as determined by XPS, EELS, and X-ray diffraction. For experiments where films were annealed in vacuo, tin oxide was sputter deposited on a Pt foil that could be resistively heated. A type K chromel–alumel thermocouple (spotwelded to the back of the foil) was used to monitor temperature.

X-ray diffraction of the sputter-deposited tin oxide films gave patterns that match with ASTM data for tetragonal SnO_2.[20] No peaks characteristic of SnO or Sn_2O_3 were observed. The relative diffracted intensities and peak widths indicated that the films were comprised of randomly oriented 200–300-Å-diameter crystallites of SnO_2.

From a measurement of photoelectron intensity as a function of emission angle of the as-deposited (sputter-deposited films exposed to atmosphere) tin oxide films, it was inferred that the as-deposited tin oxide surface roughness was significant enough to scatter photoelectrons emitted at low takeoff angles.[20] It has been pointed out that a significant amount of surface contour irregularity or roughness can complicate considerably the interpretation of AR-XPS data, because a host of different emission angles will be sampled for a given acceptance angle.[21] It was found that significantly smoother surfaces could be produced (as monitored by AR-XPS intensities) by annealing the as-deposited tin oxide films in a quartz tube furnace for 24 h at 900 °C in a flowing O_2 atmosphere followed by cooling to room temperature over 3–4 h. Thus, all sputter-deposited tin oxide films were annealed in oxygen as described above before AR-XPS analysis. X-ray diffraction of O_2 annealed films showed that the average SnO_2 crystallite diameter increased to approximately 1000 Å, indicating that sintering of the film had occurred.[20]

Tin oxide films deposited by a spray hydrolysis method on optical grade quartz plate were obtained from PPG Industries, Pittsburgh, PA. These films were cleaned by successive 30-min ultrasonic treatments in Alconox/water solution, water, isopropyl alcohol, methanol, and water. Measurement of the emitted photoelectron intensity as a function of emission angle indicated that the PPG films were smooth enough to make the O_2 annealing treatment mentioned above unnecessary for AR-XPS analysis.

Radio frequency water plasma treatments of the tin oxide films were performed in a turbomolecular pumped, ultrahigh vacuum compatible, six-way cross chamber that was isolated from the analysis chamber by a gate valve.[22] The samples were transported between the chamber housing the plasma reactor and the analysis chamber by a long-throw manipulator. Plasma treatments were conducted under flowing conditions, and a butterfly valve on the pumping line was used to throttle the gas flow. Typical plasma treatments were performed at 75–100 mT of H_2O, 1–5-W net for 10–15 min.

AR-XPS studies were performed using a Perkin-Elmer/Physical Electronics (PHI) Model 5400 electron spectrometer equipped with a Model 10-360 spherical capacitor analyzer (SCA).

(20) Tarlov, M. J. Ph.D. Dissertation, University of Minnesota, 1987.
(21) Baird, R. J.; Fadley, C. S.; Kawamoto, S. K.; Meta, M.; Alvarez, R.; Silva, J. A. *Anal. Chem.* **1976**, *48*, 843.
(22) Evans, J. F.; Gibson, J. H.; Moulder, J. F.; Hammond, J. S.; Goretzki, H. *Fresenius Z. Anal. Chem.* **1984**, *319*, 841.

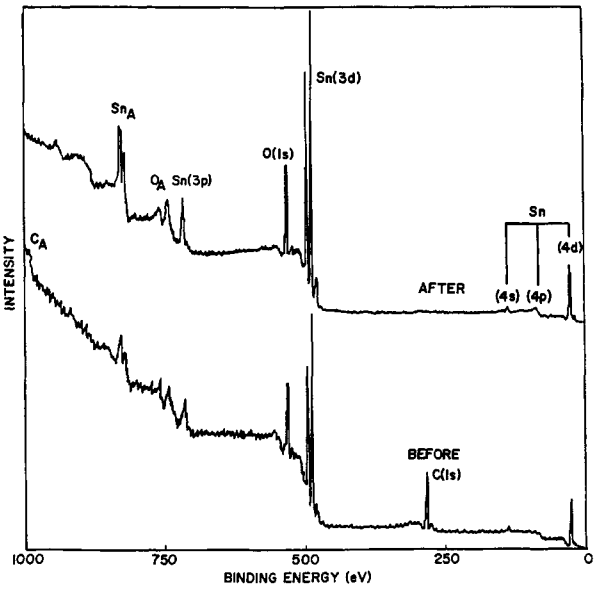

Figure 1. AR-XPS survey spectra acquired at an emission angle of 10° of a sputter-deposited tin oxide film before and after water plasma exposure.

Emission angles were defined with respect to the sample surface plane. High-resolution XPS spectra were acquired by operating the SCA at a pass energy of 17.90 eV. Angle-integrated XPS (AI-XPS) and EELS were performed using a PHI Model 555 spectrometer. High-resolution XPS and EELS spectra were acquired by operating the double-pass cylindrical mirror analyzer (CMA) in the retarding mode at a pass energy of 25 eV. Excitation for AI- and AR-XPS spectra was provided by a Mg anode operated at 14 kV, 300 W. An electron gun mounted coaxially in the CMA was used to acquire EELS spectra. The electron beam was defocused to irradiate an area of approximately 0.25 cm^2, and currents were 10^{-7} A or less. The samples were oriented such that the surface plane was at an angle of 30° with respect to the CMA axis. A PHI Model 04-303 differentially pumped ion gun was used for sputtering. A 5-keV argon ion beam was rastered over an area of approximately 1 cm^2. The angle between the ion beam and sample normal was 33°.

Results and Discussion

Water Plasma Treatment of Tin Oxide Films. Figure 1 compares the low-resolution AR-XPS spectra collected at an emission angle of 10° (more surface sensitive) of an as-deposited sputter-deposited tin oxide film before and after water plasma exposure. The effectiveness of the water plasma in removing surface carbon contamination is demonstrated by the complete disappearance of the C(1s) signal in the spectrum of the water plasma treated film. All features in the spectrum of the plasma treated film are assignable to oxygen or tin. Silicon and chromium were detected by XPS on tin oxide surfaces that were exposed to water plasmas of relatively high power (>20 W). This was attributed to sputtering of the glass and stainless steel wall material from ions accelerated across the plasma sheath. Thus, water plasma treatments were conducted at relatively low powers to avoid this undesirable effect.

Figure 2a shows the superposition of two high-resolution XPS spectra of the O(1s) region, recorded at emission angles of 10° and 90°, for a water plasma treated, sputter-deposited tin oxide film that was previously annealed ex situ in oxygen. Both O(1s) lines show broadening to higher binding energy, which has previously been assigned to adsorbed hydroxyl groups and water.[16] This interpretation is supported by static secondary ion mass spectrometry (SIMS) data acquired from similarly treated tin

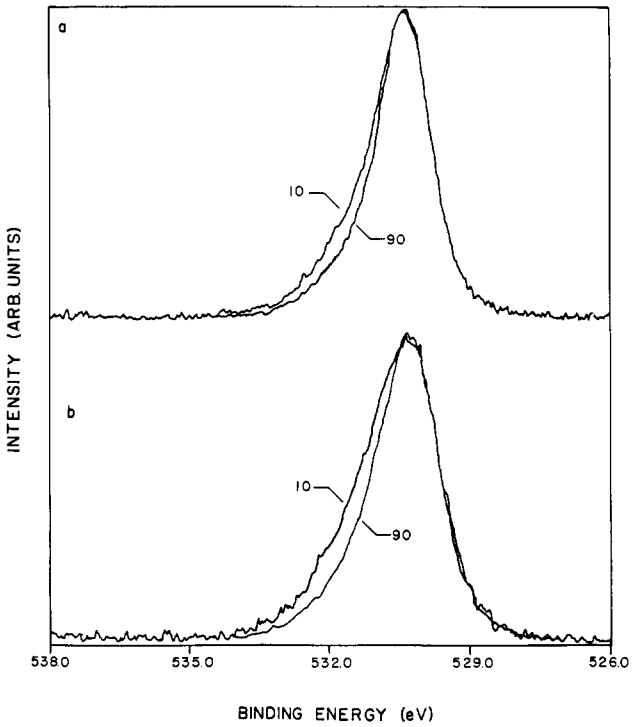

Figure 2. (a) Comparison of XPS spectra of the O(1s) region recorded at 10° and 90° emission angles of a water plasma treated sputter-deposited tin oxide film that was previously annealed at 900 °C in a flowing O_2 atmosphere for 24 h. (b) Comparison of XPS spectra of the O(1s) region recorded at 10° and 90° emission angles of a water plasma treated PPG tin oxide film.

oxide surfaces that detect OH^-, H_2O^+, and $SnOH^+$ secondary ions.[23] The greater broadening to the higher binding energy side of the 10° spectrum indicates that greater concentrations of hydroxyl groups and adsorbed water exist closer to the surface. The 10° measurement samples a mean depth that is approximately 6 times shallower than that of the 90° measurement. The peak shapes of the O(1s) line acquired at 10° and 90° before and after the water plasma treatment were almost identical for most samples. Several as-deposited films exhibited more pronounced broadening and in some cases resolvable peaks on the high binding energy side of the O(1s) line. These features were attributable to oxygen-containing carbon contamination as evidenced by higher binding energy components between 286 and 293 eV in the C(1s) high-resolution spectra. Removal of this contamination by water plasma treatment resulted in a reduction of the higher binding energy O(1s) features. This emphasizes the need to eliminate surface carbon contamination before extensively analyzing the O(1s) line shape. The 10° O/Sn ratio typically increased 5–10% after the water plasma treatment for as-deposited films with little oxygen-containing carbon contamination, while the 90° O/Sn ratio increased less than 5%. Taken in total, this indicates that small amounts of oxygen species are incorporated in the near surface region from the water plasma exposure. Also, the preservation of the O(1s) line shape implies that the oxygen species, namely, O^{2-}, OH^-, and H_2O, have increased by proportionate amounts. Similar AR-XPS results were obtained from PPG films annealed at 900 °C in oxygen prior to water plasma treatment.

Figure 2b shows the superposition of two high-resolution XPS spectra of the O(1s) region of an RF water plasma treated *unannealed* PPG tin oxide/quartz sample recorded at emission angles of 10° and 90°. As for the annealed, sputter-deposited, and PPG tin oxide films, greater broadening to the higher binding energy side is observed in the 10° spectrum, indicating that hydroxylation is more extensive closer to the surface. The conclusions drawn above concerning the incorporation of oxygen species from water plasma treatment of annealed tin oxide films can be extended to the similarly treated, unannealed PPG tin oxide films. However, the concentration of hydroxyl functionalities for the unannealed film is typically 50% higher, as indicated by curve-fitting results described below.

(23) Tarlov, M. J.; Evans, J. F., manuscript in preparaton.

Table I. Fitting Parameters for O(1s)

component[a]	Δ,[b] eV	fwhm,[c] eV
O^{2-}	0.00	1.40 ± 0.05
OH^-	1.20 ± 0.10	1.50 ± 0.05
H_2O	2.20 ± 0.10	1.70 ± 0.05

[a] The line shapes were fixed at 80% Gaussian and 20% Lorentzian. [b] The difference in binding energy with respect to the O^{2-} peak position. [c] Full width at half maximum.

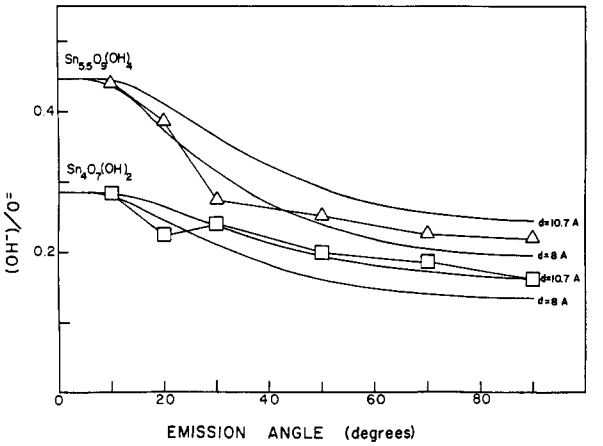

Figure 3. Plot of OH^-/O^{2-} (determined by curve fitting of the O(1s) line) XPS intensity ratios as a function of photoelectron emission angle. The triangles correspond to data from a water plasma treated PPG tin oxide film, while the squares correspond to a similarly treated PPG tin oxide film that was previously annealed at 900 °C in a flowing O_2 atmosphere for 24 h. The solid curves were generated from eq 1.

The O(1s) lines at different emission angles were curve fitted to three species (O^{2-}, OH^-, and H_2O) to obtain more quantitative information about the relative concentration and distribution of hydroxyl groups. The fitting parameters are given in Table I. When fitting the O(1s) lines of the same sample at different emission angles, the Δ and fwhm values usually did not vary more than ±0.05 eV. The deviations represent the limits set for fitting the O(1s) lines of all the different tin oxide samples. The O^{2-} fwhm and Δ values were obtained from the O(1s) line after annealing a sample in vacuo at 600 °C, thereby desorbing all water and dehydroxylating the surface. The water fwhm and Δ values were determined by condensing water onto a tin oxide surface cooled to near liquid nitrogen temperature. The OH^- fwhm and Δ values were subsequently determined by a best-fit procedure.

The curve-fitting results of the O(1s) line as a function of emission angle are represented graphically in Figure 3, where the OH^-/O^{2-} ratio (obtained by dividing the OH^- peak area by that of O^{2-}) is plotted versus the photoelectron emission angle. The solid curves were generated from a model that describes the relative OH^- and O^{2-} signal intensities as a function of emission angle. In this model it is assumed that a hydroxyl-free SnO_x substrate is cov-

ered by a uniform, partially hydroxylated overlayer $SnO_y(OH)_z$. For such a thin-film geometry it can be shown that the ratio of the OH^- and O^{2-} signal intensities, $I_{OH^-}/I_{O^{2-}}$, is given by

$$\frac{I_{OH^-}}{I_{O^{2-}}}(d,\theta) = \frac{\beta_{OH^-}[1 - \exp(-(d/\lambda \sin \theta))]}{(1 - \beta_{OH^-}) + \beta_{OH^-} \exp(-(d/\lambda \sin \theta))} \quad (1)$$

where θ is the emission angle, d is the hydroxylated layer thickness, β_{OH^-} is the fraction of oxygen existing as OH^-, and λ is the mean free path of the O(1s) photoelectrons.[20] The assumptions used in deriving eq 1 are (1) the photoelectric cross sections for O^{2-} and OH^- are equal, (2) the mean free path in the hydrated layer and the oxide substrate are equal, and (3) both layers are uncharged and the tin in these layers exists in the fully oxidized +4 state. VB-XPS and EELS data presented below show the water plasma treated surfaces possess Sn^{4+} valency. A value of 11 Å was used for the mean free path of the O(1s) photoelectrons (kinetic energy ~715 eV) in tin oxide.[24]

As can be seen from Figure 3, the annealed tin oxide surface is hydroxylated to a lesser extent than the unannealed surface after the same treatment. The 10° measurement and curve fit give a value of 0.28 for OH^-/O^{2-}, which corresponds to a hydrated layer stoichiometry of $Sn_4O_7(OH)_2$. Using a β_{OH^-} value of 0.22 and a hydrated layer thickness of 10 Å, eq 1 fits the data well. The annealed, water plasma treated, sputter-deposited tin oxide films yield almost identical results. The unannealed water plasma treated PPG tin oxide film shows greater surface hydroxylation with $OH^-/O^{2-} = 0.45$, which corresponds to a hydrated layer stoichiometry of $Sn_{5.5}O_9(OH)_4$ and a β_{OH^-} value of 0.31. A hydrated layer thickness of 8–10 Å fits these data well.

The greater hydroxylation of the unannealed water plasma treated film was expected. It is likely that the high-temperature oxygen annealing results in dehydroxylation of the tin oxide surface, accompanied by reconstruction of the exposed surface crystal planes.[25] The oxidized (110) surface of single-crystal SnO_2 has been found to be nearly inert to exposure to gas-phase water at room temperature.[26] Hydroxylation of the oxygen-annealed tin oxide surface occurs from either atmospheric and/or water plasma treatment. In the absence of gross carbon contamination, the O(1s) line shape is identical before and after plasma treatment, indicating that the water plasma does not induce massive hydroxylation of the surface or bulk.

There have been various reports of the thickness of a hydrated layer on polycrystalline tin oxide ranging from 6 to 30 Å.[14] Our results for the unannealed PPG tin oxide film exposed to atmospheric humidity for approximately 7 years following preparation fall on the low side of this range at an estimated 10 Å. The reasons for the variability are likely to reflect variability in defect density on the surface; the defects (oxygen vacancies) being the likely sites for the dissociative adsorption of water leading to the surface hydroxyl groups. These defect density variations could then be directly related to the method of preparation and thermal history of the samples under study.

Egashira et al. have determined surface hydroxyl coverages from chromatographic temperature-programmed desorption (TPD) experiments performed on high surface area tin oxide powders.[25] The experimentally determined surface hydroxyl coverages were compared with those calculated from crystallographic models assuming that water adsorbs dissociatively on various stoichiometric cleavage planes of SnO_2 to *saturation* coverages. In Table II the surface hydroxyl coverages calculated by Egashira et al. are compared with the coverages obtained in the present study from the AR-XPS data. With use of an average unit cell area from the 110, 100, 101, and 001 surface crystal planes of 21.5 Å^2, the PPG annealed and unannealed tin oxide surfaces exhibit coverages of 2.3×10^{14} and 3.4×10^{14} OH/cm^2, respectively. These surface hydroxyl coverages are approximately 4–6 times lower than the calculated hydroxyl surface density if an average value of 1.4×10^{15} OH/cm^2 is taken for the four low-index tin oxide crystal planes. In comparison, Egashira et al. determined a hydroxyl coverage of approximately 1×10^{15} OH/cm^2 in their work. It is interesting to note that for colloidal tin oxide systems, a wide range of values has been reported for the surface density of ionizable protons, which can roughly be equated with the hydroxyl coverage. Data from acid/base potentiometric titrations of high surface area powders have yielded values of 4×10^{10}, 1×10^{13}, 2×10^{14}, and 3×10^{14} OH/cm^2.[27-30] The discrepancy between these titrimetric results may be due to the various synthetic procedures used to prepare these samples.

Table II. Calculated and Experimental Hydroxyl Coverages on SnO_2 Surfaces

surf. cryst plane	stoichiometry	OH^-/O^{2-}	unit-cell area, Å^2	surf. OH/cm^2
110	$Sn_2O_3(OH)_2$	0.67	21.3	9.4×10^{14}
100	$SnO(OH)_2$	2.00	15.1	1.3×10^{15}
101	$SnO(OH)_2$	2.00	27.0	1.5×10^{15}
001	$Sn(OH)_4$		22.4	1.8×10^{15}
	$Sn_{5.5}O_9(OH)_4$[a]	0.44	21.5[c]	3.4×10^{14}
	$Sn_4O_7(OH)_2$[b]	0.29	21.5[c]	2.3×10^{14}

[a] Experimental data from angle resolved XPS, water plasma treated unannealed PPG tin oxide. [b] Experimental data from angle-resolved XPS, water plasma treated PPG tin oxide previously annealed for 24 h, O_2 atmosphere, 900 °C. [c] Average unit cell area from 110, 100, 101, and 001 surface crystal planes.

There are a number of explanations why the hydroxyl coverages determined in this study are considerably smaller than those calculated by Egashira et al. for a fully hydroxylated tin oxide surface. Examination of space-filling models for different rutile surfaces shows that full hydroxylation would result in very high hydroxyl packing densities. Of course, the hydroxyl group possesses an electric dipole. High hydroxyl surface coverages might result in substantial repulsive dipole–dipole interactions. This destabilization could be the driving force for surface reconstruction processes. This is similar to the so-called "place-exchange" model that was formulated to explain the surface roughening of platinum from electrochemical oxidation.[31]

Another questionable assumption used in the calculation of the hydroxyl coverages is that water adsorbs dissociatively on the different surface crystal planes, resulting in the formation of hydroxyl functionalities. Only very weak adsorption of water at room temperature, if any at all, on

(24) Cox, P. A.; Egdell, P. G.; Harding, C.; Patterson, W. R.; Tavener, P. J. *Surf. Sci.* **1982**, *123*, 179.
(25) Egashira, M.; Nakashima, M.; Kawasumi, S.; Seiyama, T. *J. Phys. Chem.* **1981**, *85*, 4125.
(26) Cox, D. F.; Fryberger, T. B.; Semancik, S. *Phys. Rev. B* **1988**, *38*, 2072.
(27) Huang, C. P. Ph.D. Dissertation, Harvard University, 1971.
(28) Ray, K. C.; Khan, S. *Indian J. Chem.* **1978**, *16*, 12.
(29) Boehm, H. P. *Discuss. Faraday Soc.* **1971**, *52*, 264.
(30) Ahmed, S. M.; Maskimov, D. J. *J. Colloid Sci.* **1969**, *29*, 97.
(31) Angerstein-Kozlowska, H.; Conway, B. E.; Sharp, W. B. E. *J. Electroanal. Chem.* **1973**, *43*, 9.

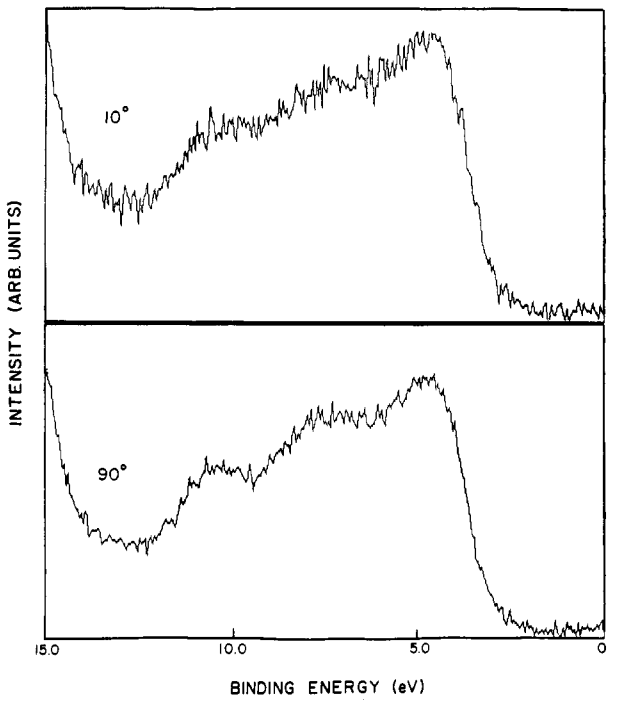

Figure 4. XPS-VB spectra acquired at emission angles of 10 and 90° of an unannealed PPG tin oxide film that has been exposed to a water plasma.

in vacuo annealed and Ar^+-bombarded tin oxide surfaces was observed in this laboratory. Similar findings have been reported by using UPS to monitor water adsorption on oxygen deficient polycrystalline tin oxide surfaces.[32] The adsorption of water on an annealed (110) SnO_2 surface at 90 K has been examined, and it was concluded that adsorption was molecular.[33] In general it has been found that well-ordered metal oxide single crystal samples are inert to gas-phase water, and it has been suggested that dissociation of water on high surface area powders occurs primarily at defect sites and facet edges.[34,35]

Figure 4 shows VB-XPS spectra acquired at emission angles of 10° and 90° of an unannealed PPG tin oxide film that has been exposed to an rf water discharge. The surface stoichiometry of this sample is $Sn_{5.5}O_9(OH)_4$, which was determined by the O(1s) fitting procedure previously described. Both spectra are very similar to the SnO_2 VB-XPS spectrum reported by Lau and Wertheim.[17] Therefore, the surface appears to be in the fully oxidized Sn^{4+} state. This interpretation is supported by the EELS spectra acquired from a similarly treated surface that are presented later.

The assignments of the features in the spectra follow those made for UPS spectra of polycrystalline[32] and single-crystal (110) tin oxide surfaces.[36] The features between 0 and 14 eV of binding energy arise primarily from photoemission from O(2p) valence band states. The most intense feature at 5 eV is due to the O(2p) lone-pair, nonbonding orbitals. These are oriented perpendicular to the Sn–O bond axis and, therefore, stabilized the least by the Sn^{4+} cations. The feature centered at 7.5 eV is thought to be due to minimally bonding O(2p) orbitals with a small Sn(5p) admixture. The feature centered at 10.5 eV is assigned to the bonding O(2p) orbitals that are directed toward the Sn^{4+} nearest neighbor cations.

VB-XPS spectra of polycrystalline tin oxide surfaces have been reported that show a large increase in the relative intensity of the feature at approximately 10 eV.[14] This was associated with a thoroughly hydrated SnO_2 surface arising from exposure to atmospheric humidity. From UPS studies the 3σ valence orbital of metal hydroxide is expected to have a binding energy between 9 and 11 eV.[34] The VB-XPS spectra in Figure 4 do not exhibit a relatively intense feature at 10 eV that can be definitively associated with adsorbed hydroxyl group. Moreover, the high degree of similarity between the 10° and 90° XPS-VB spectra is noteworthy, because it suggests that hydroxylation of the tin oxide surface, at least to the extent reported here, does not substantially perturb the surface electronic structure.

EELS, like VB-XPS, was used as a qualitative technique in this study. Powell was the first to demonstrate that stannic oxide (SnO_2) and stannous oxide (SnO) can be distinguished by their EELS spectra.[18] Recently, an interpretation of EELS spectra obtained from annealed, Ar^+-sputtered, and O_2-treated polycrystalline tin oxide films, prepared by a spray hydrolysis method, was given.[37] EELS was used here to examine the effects of water plasma treatment on tin oxide surfaces, and these spectra are compared to those reported previously.

Figure 5, top, shows EELS spectra of an as-deposited tin oxide film collected at electron primary beam energies of 1000, 500, and 200 eV. The elastic peak of each spectrum, which defines the energy zero, is omitted. Shown in the inset are EELS spectra from Powell's work of Sn, SnO, and SnO_2 collected at a primary beam energy of 400 eV. Different sample depths are probed by varying the primary beam kinetic energy. Decreasing the energy leads to a reduction in the electron mean free path (MFP $\sim$ $(KE)^{1/2}$); therefore, the EELS spectrum collected at low primary beam energy is more representative of the surface. Conversely, higher beam energies produce spectra more representative of the bulk. (This assumes that the cross sections for the electronic transitions giving rise to the energy losses remain relatively constant with primary beam energy.) The main loss feature at 20 eV is characteristic of SnO_2 by comparison to Powell's work. As the primary beam energy is decreased (more surface sensitive), the loss feature at approximately 28 eV grows relative to the main loss feature. From Powell's work, the 28 eV feature is indicative of SnO. Its relative increase with decreasing beam energy suggests SnO is located nearer the surface. This is supported by the relative increase in the features between 8 and 10 eV, which is also found in Powell's SnO EELS spectrum, with decreasing beam energy. There is also a corresponding decrease in the features between 30 and 40 eV, which have been proposed to directly correlate with oxygen concentration.[37] An oxygen deficiency is consistent with a SnO surface stoichiometry.

It is stressed that the observed SnO loss features are *not* a consequence of electron beam damage. It has been reported from mass spectrometric, AES, and conductivity measurements that electron bombardment of tin oxide causes surface dissociation and subsequent desorption of oxygen.[38] Those studies were performed with high beam currents (100 μA, irradiated area not reported) and voltage (2 keV). Electron beam induced damage was avoided in

(32) Cox, D. F.; Semancik, S.; Szuromi, P. D. Proceedings of the International Conference on Solid-State Sensors and Actuators-Transducers, 1985; p 385.
(33) Cox, D. F.; Semancik, S.; Szuromi, P. D. *J. Vac. Sci. Technol.* **1986**, *A4*(3), 626.
(34) Thiel, P. A.; Madey, T. E. *Surf. Sci. Rep.* **1987**, *7*, 211.
(35) Henrich, V. E. *Rep. Prog. Phys.* **1985**, *48*, 1481.
(36) Egdell, R. G.; Eriksen, S.; Flavell, W. R. *Solid State Commun.* **1986**, *60*, 835.
(37) Cox, D. F.; Hoflund, G. B. *Surf. Sci.* **1985**, *151*, 202.
(38) Shapira, Y. *J. Appl. Phys.* **1981**, *52*, 5696.

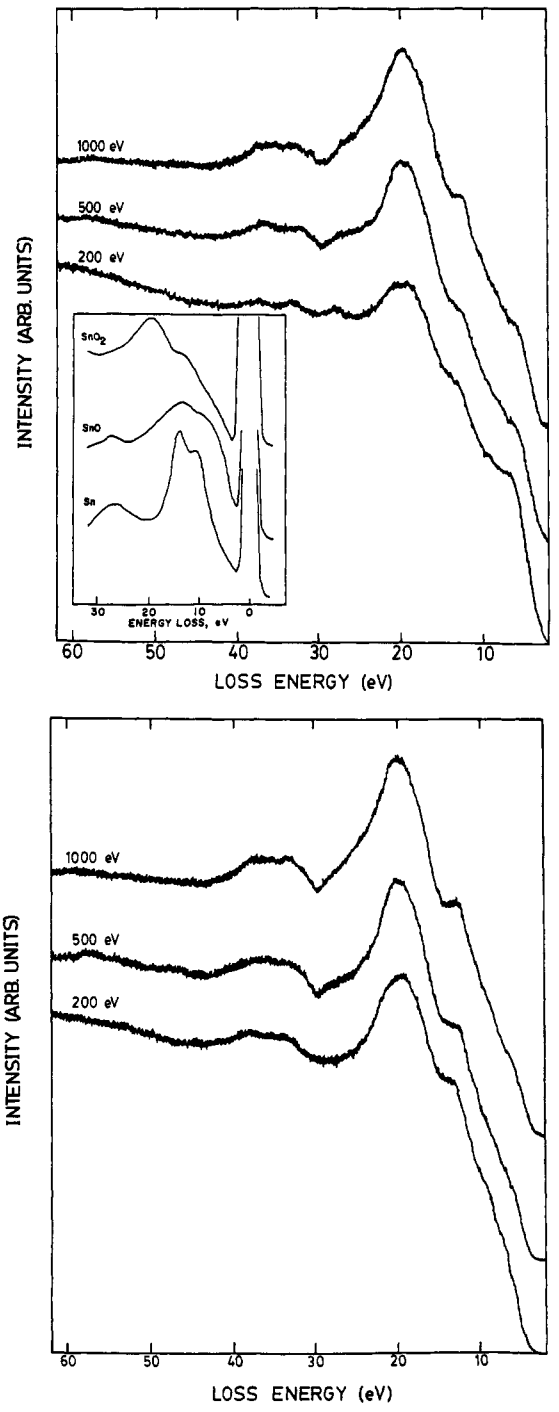

Figure 5. Top: EELS spectra of an "as-deposited" tin oxide film acquired with electron primary beam energies of 200, 500, and 1000 eV. Shown in the inset are EELS spectra from ref 18 of Sn, SnO, and SnO_2 collected at a primary beam energy of 400 eV. (b) EELS spectra of a water plasma treated sputter-deposited tin oxide film acquired with electron primary beam energies of 200, 500, and 1000 eV.

this work by using a defocused primary beam to irradiate a relatively large sample area (~0.25 cm^2), thereby decreasing the beam flux, and by using beam currents of 10^{-7} A/cm^2 or less. The EELS spectra were always collected by using the lower primary beam energies (more surface sensitive) first. EELS spectra presented below of water plasma treated samples demonstrate that electron beam effects are negligible in this operating mode.

EELS spectra acquired from as-deposited tin oxide films generally indicated a surface stoichiometry of SnO. This is thought to be due to heating of the growing film during the sputter deposition from electron and ion bombardment. The films, which reached a maximum temperature at the termination of sputtering, were allowed to cool for 1 h in the vacuum chamber at the completion of the deposition. It is well-known that vacuum annealing induces the desorption of oxygen from tin oxide surfaces.[24,26] Evidently the SnO surface stoichiometry of the deposited films is largely preserved when the films are exposed to atmosphere at room temperature. EELS spectra of oxygen-annealed sputter-deposited tin oxide films are similar to those in Figure 5, top, except that SnO features are not present. It has been shown that a relatively high temperature (400 °C) and pressure (1 Torr of O_2) treatment is necessary to produce a nearly ideal stoichiometric $SnO_2(110)$ surface.[26]

EELS spectra recorded at primary beam energies (E_p) of 200, 500, and 1000 eV of an rf water plasma treated, unannealed, sputter-deposited tin oxide film are presented in Figure 5, bottom. In comparison to the EELS spectra of the as-deposited film in Figure 5, top, the salient features of these spectra may be summarized as follows. The main loss feature centered at 20 eV is sharpened somewhat, particularly in the 200-eV spectrum. This may be due in part to elimination of the hydrocarbon overlayer through which inelastic scattering occurs. The feature located between 6 and 10 eV in Figure 5, top, which increases in relative intensity as the beam energy decreases, is almost absent as a result of water plasma treatment. This is particularly true of the spectrum at E_p = 200 (more surface sensitive). As mentioned previously, the 28-eV feature is characteristic of SnO.[18,37] This indicates that water plasma exposure has converted that component of the surface in the Sn^{2+} state to the higher Sn^{4+} valency. Examination of the loss features located between 30 and 40 eV supports this contention. These features are more prominent in the spectra of the water plasma treated tin oxide film, particularly in the E_p = 200 eV spectrum, than in the spectra of the as-deposited film. An increase in the relative intensity of these features is expected, if they are related to oxygen concentration as has been proposed, because oxygen incorporation would likely accompany an increase in the tin oxidation state to maintain electroneutrality at the surface.[37] Not that the absence of the 28-eV feature strongly suggests that the SnO feature present in the spectra of the as-deposited tin oxide film is not an artifact of electron beam damage.

Cox and Hoflund assign the major features in the tin oxide energy loss spectrum to collections of optically or dipole allowed ($\Delta l \pm 1$) interband transitions from occupied to unoccupied states.[37] The features below 28 eV are assigned to dipole allowed valence band (VB) to conduction band (CB) transitions, while the features at and above 28 eV are assigned to dipole-allowed core level (O(2s) or Sn(4d)) to CB transitions. The 28-eV loss feature is interpreted as an Sn(4d) to CB minimum transition.[39] It is thought that this feature is not observed in SnO_2 because the CB minimum, which is empty for defect-free SnO_2, is mostly Sn(5s)-like and, therefore, a Sn(4d) to CB minimum transition is dipole unallowed. When SnO_2 is reduced to SnO, population of the Sn(5s) states occurs. The CB minimum, or lowest unoccupied state, then becomes more Sn(5p)-like. Thus, a Sn(4d) to CB minimum transition is dipole allowed for SnO, and this translates to the appearance of a 28-eV energy loss feature.

Cox and Hoflund assign the loss features centered at 36 eV to O(2s) to CB transitions. This is consistent with the

(39) Bevolo, A. J.; Verkoeven, J. D.; Noack, M. *J. Vac. Sci. Technol.* **1982**, *20*, 943.

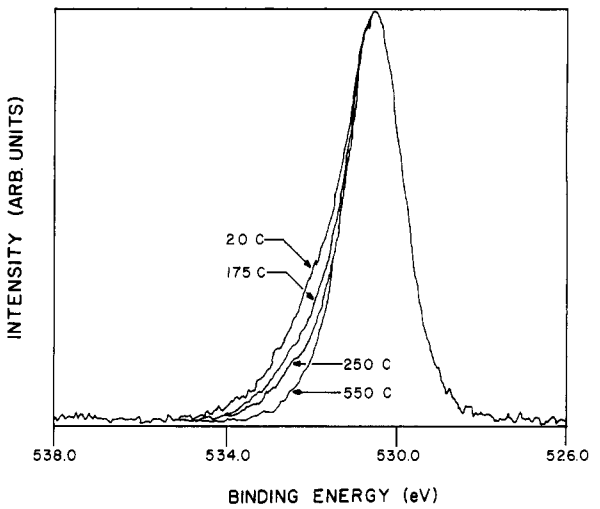

Figure 6. Superposition of high-resolution AI-XPS spectra of the O(1s) region acquired from a sputter-deposited tin oxide film annealed in vacuo at various temperatures. Prior to annealing, the film was exposed to a water plasma.

decrease in intensity of this feature associated with more oxygen deficient tin oxide surfaces and vice versa. Presumably the final state(s) involved is (are) mostly Sn(5p)-like, because coupling to a Sn(5s)-like state would be dipole unallowed.

The EELS results presented above are in general agreement with those reported by others.[18,37] Two prominent loss features observed by others, however, are not present in the EELS spectra given above. It has been suggested that one of the features (~45 eV) is sensitive to structural defects in the surface region while the other (between 23 and 29 eV) is indicative of a well-hydrated tin oxide surface.[14,37] We have been able to reproduce these features at similar loss energies and relative intensities in our laboratory by varying the emission setting of the electron gun used to excite the spectra.[20] Thus, we believe that these loss features reported previously are most likely due to an instrumental artifact associated with the electron gun. More specifically, a lower energy and intensity component of the primary beam is generated at certain emission settings that appears as a peak in the loss spectrum. This anomalous feature was observed to shift as the emission setting was varied and to decrease in intensity with decreasing beam voltage.[20] In addition, no loss features that can be related unambiguously to adsorbed hydroxyl groups have been observed by us, at least to the extent of tin oxide surface hydroxylation reported here.

Annealing of Water Plasma Treated Tin Oxide Films. In all of the annealing experiments no changes were observed in the Sn(3d) line shapes, and for this reason they are not presented. The O(1s) line, which was shown earlier to be comprised of components due to hydroxyl functionalities and adsorbed water, did change as expected and, therefore, the majority of data presented are of the O(1s) region.

Figure 6 shows the superposition of angle integrated O(1s) spectra acquired from a sputter-deposited tin oxide film annealed in vacuo. Prior to annealing, the film was exposed to an rf water plasma, which removed all XPS-detectable carbon contamination. The spectra, normalized to the plasma-treated O(1s) peak height, were collected after water plasma treatment and subsequent annealing for 30 min at 175, 250, and 550 °C. The higher binding energy shoulder decreases in relative intensity as the annealing temperature increases, indicating a gradual loss of adsorbed water and surface hydroxyl functionalities.

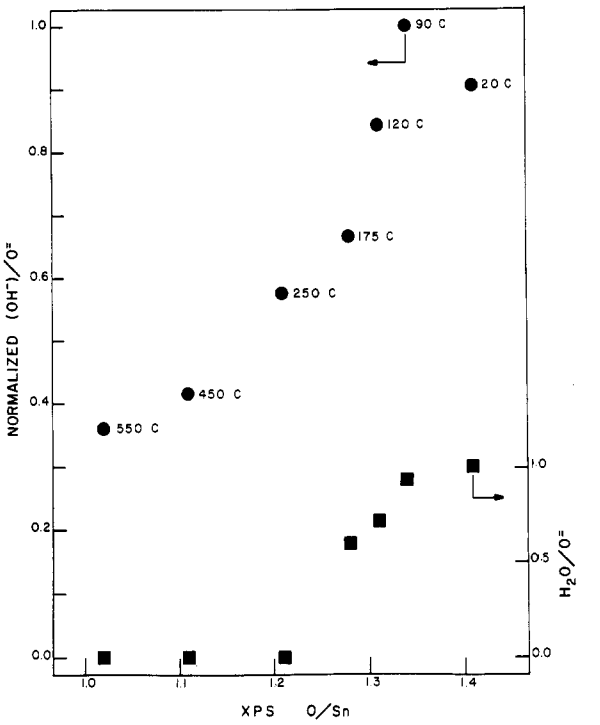

Figure 7. Plot of the normalized OH^-/O^{2-} ratios, determined from curve fitting of the O(1s) line shape, as a function of the AI-XPS O/Sn ratio for a sputter-deposited tin oxide film annealed in vacuo at various temperatures. The H_2O/O^{2-} (■) and OH^-/O^{2-} (●) intensities are represented proportionally in the figure.

This is consistent with static SIMS data acquired after each annealing step that show a corresponding decrease in OH^-, H_2O^+, and $SnOH^+$ relative signal intensities.[23] This is also reflected in the O/Sn ratio determined by XPS, which decreases from 1.41, for the water plasma treated surface, to 1.02 after annealing at 550 °C for 30 m. The O(1s) exhibits little asymmetry after annealing at 550 °C, indicating almost complete dehydroxylation of the surface.

Figure 7 is a plot of the normalized OH^-/O^{2-} and H_2O/O^{2-} ratios (determined from curve fitting of the O(1s) line shape) as a function of the XPS-determined O/Sn ratio. The fitting parameters used were the same as those used for the angle-resolved data (see Table I). The amount of adsorbed water decreases gradually between 20 and 175 °C. Adsorbed water is completey removed after treatment at 250 °C. Surprisingly, the OH^-/O^{2-} ratio also decreases between 20 and 250 °C. The onset temperature for dehydroxylation of high surface area tin oxide powders, determined by TPD, has been reported to be between 200 and 250 °C.[25,40] These powders were hydroxylated by exposure to water vapor. The existence of seemingly labile surface hydroxyl groups is rationalized by postulating that exposure of the tin oxide surface to a water plasma results in the formation of metastable hydroxyl functionalities.

Figure 8 shows EELS spectra acquired by using primary beam energies (E_p) of 200, 500, and 1000 eV from a sputter-deposited tin oxide film that was successively rf water plasma treated and annealed in vacuo at 550 °C for 1 h. The spectra clearly demonstrate that the near surface region has undergone a partial reduction to a more SnO-like material as a result of the annealing step. This is in agreement with the VB-XPS results. The 13- and 28-eV loss features, which are both characteristic of SnO, increase

(40) Giesekke, E. W.; Gutowsky, H. S.; Kirkov, P.; Laitinen, H. A. *Inorg. Chem.* **1967**, *6*, 1294.

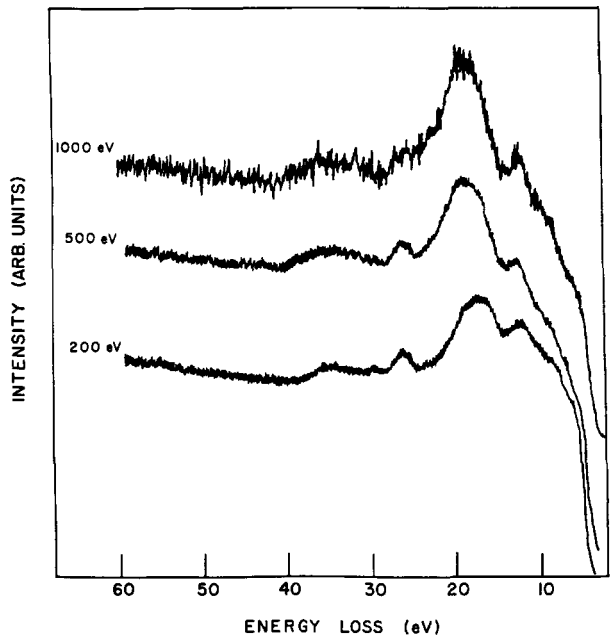

Figure 8. EELS spectra acquired from a sputter-deposited tin oxide sample that was successively water plasma treated and annealed in vacuo at 550 °C for 1 h. Electron primary beam energies of 200, 500, and 1000 eV were used.

in relative intensity as E_p decreases. Also, the shoulder between 6 and 10 eV is much more prominent in the E_p = 200 eV spectrum. The loss features centered at 35 eV decrease in relative intensity as E_p decreases. It is interesting to note that the centroid of the main loss peak for SnO_2 in the E_p = 200 eV spectrum is shifted to approximately 2 eV lower loss energy in comparison to the same feature in the E_p = 1000 eV spectrum. This probably indicates that the SnO_2 electronic structure is perturbed only at or nearer to the surface. This is supported by examination of the more bulk sensitive E_p = 1000 eV spectrum, which shows little change in the shape or position of the main SnO_2 loss feature compared to that of the plasma-treated film.

The EELS spectra presented above are in qualitative agreement with those reported previously for similarly annealed tin oxide films with the exception of the anomalous loss feature at 46 eV.[37] AR-XPS shows that high-temperature annealing induces an oxygen deficiency that extends into the bulk at least as far as the O(1s) photoelectron sampling depth. This casts doubt on the validity of using the relative intensity of the features centered at 35 eV as an indicator of oxygen concentration. In this regard, a thorough EELS investigation of stoichiometric SnO would prove valuable.

Annealing tin oxide in vacuo produces an oxygen-deficient surface. For the sake of comparison, it is worthwhile to examine the effects of argon ion bombardment because the preferential sputtering of oxygen also produces a substoichiometric SnO_2 surface.[41-43]

EELS spectra of a tin oxide surface that has received an ion dose of 5×10^{16} Ar^+/cm^2 at 5 keV are shown in Figure 9. It is obvious that reduction of the surface to a more SnO-like material has occurred as a result of exposure to the ion beam. The more surface sensitive E_p = 200 eV spectrum shows the most dramatic changes. The loss features at 9 and 13 eV, which are characteristic of SnO, are as intense as the main SnO_2 valence band loss feature at 15.5 eV. Also, the core level loss feature at 27 eV, which is characteristic of SnO, is particularly sharp. The relative intensity of the core level features centered at 35 eV is lower, especially between 35 and 40 eV. This is expected if these features arise from a core level O(2s) to valence band transition. The relatively low O/Sn ratio of 0.76 determined by XPS confirms that oxygen has been preferentially sputtered from the tin oxide surface. As the primary beam energy increases, the relative contribution of the characteristic SnO features decreases. Ion bombardment damage is expected to be more extensive nearer the surface, and the formation of SnO-like states is likely to scale with the damage process. In addition, the main SnO_2 valence band loss feature appears at higher loss energies and becomes sharper as E_p increases. The highly disordered surface region certainly influences the density of both occupied valence band and unoccupied conduction band states between which electronic coupling occurs. The multitude of different bonding geometries in a quasiamorphous region would give rise to a broad distribution of electronic states, which would account for the observed broadening of the loss features.[37]

The lattice damage caused by Ar^+ ion bombardment can be repaired by high-temperature annealing of the tin oxide film. EELS spectra of the Ar^+-sputtered tin oxide surface after annealing in vacuo at 500 °C for 2 h are very similar to those in Figure 8 of a tin oxide film that was successively water plasma treated and annealed at 550 °C for 1 h. Thus, the main SnO_2 loss feature is sharper and shifted to higher loss energy (ca. 19 eV) in all of the spectra, implying that reconstruction to a more crystalline SnO_2-like phase has occurred as a result of the annealing step. Cox and Hoflund have reported similar findings using EELS.[37] The return to a more SnO_2-like material is supported by an increase in the XPS O/Sn ratio to 0.96. This type of behavior has been observed by others and is thought to be due to diffusion of oxygen from the bulk to the surface.[26,41-43] Also, the decrease in relative intensity of the 27-eV feature, which is characteristic of SnO, is consistent with this interpretation. The loss features centered at 35 eV increase in relative intensity, especially those between 35 and 40 eV. If these features are related to the surface oxygen concentration, this behavior is expected.

RF Water Plasma Treatment of in Vacuo Annealed Tin Oxide Films. The previous section demonstrates that in vacuo annealing of a water plasma treated tin oxide film alters the surface in a number of ways: (1) all water is desorbed between 175 and 250 °C; (2) progressive dehydroxylation of the surface occurs, although some hydroxyl functionalities remain even after heating to 600 °C; (3) the elimination of oxide oxygen and/or hydroxyl groups induces a partial reduction of the near surface region. This section examines and discusses the effects of exposing an in vacuo annealed tin oxide film to an rf water plasma. It is shown that this exposure in effect regenerates the "original" water plasma treated surface as monitored by XPS and EELS. Ion-bombarded surfaces may also be regenerated; however, they must be annealed before water plasma treatment to recrystallize the damaged surface region. If an unannealed, sputtered film is exposed to the plasma, the damaged surface region is completely converted to the Sn^{4+} oxidation state concurrent with incorporation of oxygen species; however, its amorphous character is retained.

Much of the XPS and EELS data obtained from the in vacuo annealed, water plasma treated films are identical

(41) deFresart, E.; Darville, J.; Gilles, J. M. *Appl. Surf. Sci.* **1982**, *11/12*, 637.
(42) deFresart, E.; Darville, J.; Gilles, J. M. *Solid State Commun.* **1981**, *37*, 13.
(43) deFresart, E.; Darville, J.; Gilles, J. M. *Surf. Sci.* **1983**, *126*, 518.

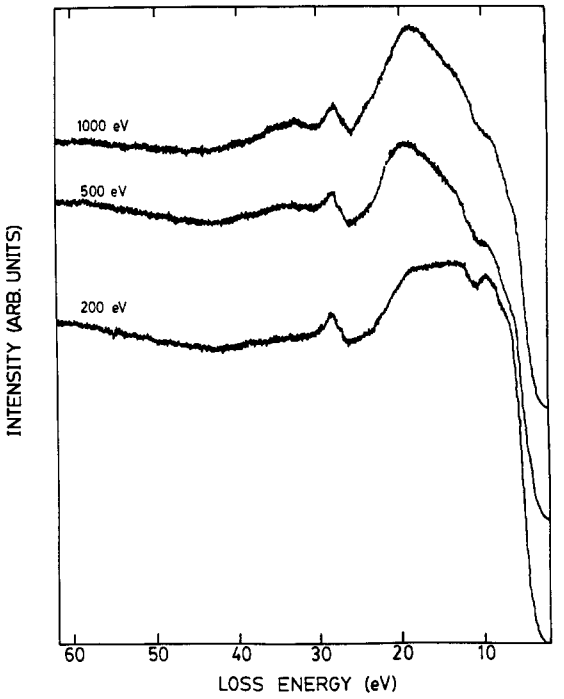

Figure 9. EELS spectra acquired with primary beam energies of 200, 500, and 1000 eV from a sputter-deposited tin oxide film that received a 5-keV ion dose of 5×10^{16} Ar^+/cm^2.

with those acquired from the "original" water plasma treated films and, therefore, have not been presented. The results from each technique are discussed collectively.

The EELS spectra acquired from a water plasma treated tin oxide film, which was previously annealed in vacuo at 550 °C for 1 h and allowed to cool to room temperature, are identical with those obtained from the plasma-treated film before annealing (see Figure 5, bottom; henceforth referred to as the original film or surface), comparing, of course, only spectra recorded with the same electron primary beam energy. The equivalence of spectra at all primary beam energies indicates that complete restoration of the electronic structure over all sampling depths has occurred as a result of the plasma treatment. The VB-XPS spectra taken at emission angles of 10° and 90° from similarly treated film also are identical with those from the original tin oxide film (see Figure 4). Thus, the VB-XPS and EELS data are in total agreement with each other, and it may be concluded that water plasma treatment of the annealed tin oxide film reverts the surface region to the fully oxidized Sn^{4+} state.

The regeneration of the original surface electronic structure requires that a number of chemical processes occur. It was shown earlier tha in vacuo annealing at high temperatures produces surface oxygen vacancies or point defects which, in turn, are manifested by spectroscopically observable Sn^{2+} electronic states. The vacancies in the surface plane are thought to exist at low-lying occupied bandgap levels.[24,26,36] Subsurface or bulk oxygen vacancies, on the other hand, act as shallow donors and are ionized at room temperature. EELS and VB-XPS spectra acquired from films that have been annealed in vacuo and then water plasma treated are characterized by the lack of Sn^{2+} features. The water plasma environment has effected the oxidation of surface Sn^{2+} to Sn^{4+}. A change in the charge state of a metal cation requires either a removal or addition of oxygen species so that electrostatic neutrality is maintained. In this case, the oxidation to the higher Sn^{4+} valence state necessitates the incorporation of oxygen or oxygen-containing species.

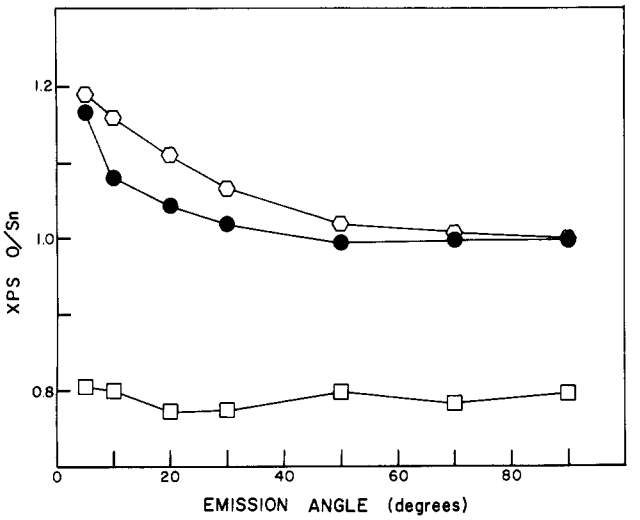

Figure 10. Plot of the XPS-determined O/Sn ratio as a function of emission angle for a sputter-deposited tin oxide film that has been subsequently water plasma treated (●), annealed in vacuo at 550 °C for 45 m (□), and water plasma treated again (○).

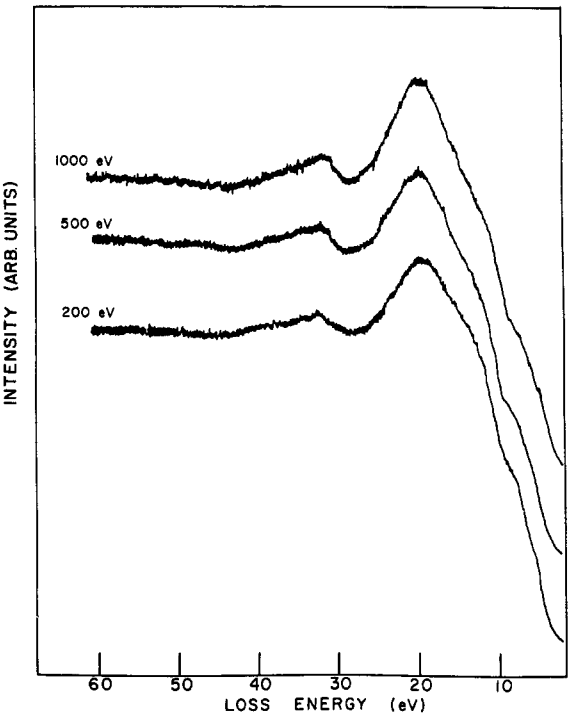

Figure 11. EELS spectra acquired at primary beam energies of 200, 500, and 1000 eV from a sputter-deposited tin oxide sample that was ion bombarded (2.5×10^{16} Ar^+/cm^2 at 5 keV) and then water plasma treated.

Angle-resolved XPS spectra of an in vacuo annealed tin oxide film before and after water plasma treatment demonstrate that incorporation of oxygen species occurs not only at, but also below, the surface. Figure 10 shows a plot of relative O/Sn XPS intensity ratios as a function of emission angle for a tin oxide film that has been subsequently water plasma treated (circles), annealed in vacuo at 550 °C for 45 min (squares), and water plasma treated again (hexagons). The O/Sn ratio measured at 5° (surface sensitive) decreases 30–35% following high-temperature annealing, as expected; however, a relatively constant O/Sn ratio of 0.80 is observed at all emission angles. The invariance of the O/Sn ratio with emission angle suggests that oxygen vacancies are not strictly confined to the surface plane but extend at least to a depth on the order

of 1 mean free pathlength. Plasma treatment of the annealed film results in an increase in the O/Sn ratio measured at each angle to approximately the same value it had before annealing. This treatment also regenerates the original O(1s) line shape at each emission angle. Therefore, plasma treatment of the annealed film results in the incorporation of both lattice oxygen and hydroxyl functionalities, along with a small amount of adsorbed water. In addition, the same relative oxide oxygen and hydroxyl stoichiometry that existed after the first water plasma treatment is restored. This suggests that the relatively deep oxygen vacancies are filled, or repaired, with oxide oxygen and not hydroxyl groups.

It should be emphasized that ignition of a plasma is necessary to oxidize the annealed tin oxide film. No oxygen incorporation or adsorption of water was observed for films exposed to 5×10^7 langmuirs of water. The dissociative adsorption of water on this surface is surely an activated process. The water plasma environment is known to be an extremely oxidative one from its efficiency in etching polymers.[19] Both atomic oxygen and hydroxyl radicals are known to be present in the water plasma. It would not be surprising if the reaction between one of these species and a Sn^{2+} surface state has a low activation barrier, if any.

It is enlightening to examine the effects of exposing an oxygen-deficient tin oxide surface prepared by Ar^+ ion bombardment to a water plasma. The annealed surfaces considered above, although polycrystalline in nature, do possess long-range structural order within individual crystallites. In contrast, tin oxide surfaces bombarded with medium-energy ions (>1 keV) are highly disordered and defect laden. This is manifested in their EELS and VB-XPS spectra, which exhibit relatively broad and shifted features. It was shown above that water plasma exposure of a tin oxide film containing surface and subsurface defects produced by high-temperature annealing results in the "gentle" addition of oxygen and elimination of these defects. This raises the question of whether an ion-sputtered tin oxide surface can be similarly repaired.

Figure 11 shows EELS spectra acquired from a tin oxide surface that was ion bombarded (2.5×10^{16} Ar^+/cm^2 at 5 keV) and then exposed to a water plasma. The XPS determined O/Sn ratio after sputtering was 0.79, and an increase to 1.26 as a result of water plasma treatment was observed. The 27-eV loss feature is absent in all the spectra, suggesting that water plasma exposure has eliminated all SnO-like material in the near surface region. This is supported by the increase in the O/Sn ratio. The position of the main energy loss feature, which occurs between 19 and 20 eV in all of the spectra, is characteristic of a SnO_2-like surface region. However, this feature is relatively broad when compared to the corresponding feature in EELS spectra of water plasma treated films that have not been subjected to ion bombardment (see Figure 5, bottom). The relative width of the main SnO_2 loss feature, and for that matter all other loss features, can be attributed to the amorphous character imparted to the surface by the sputtering process. Water plasma treatment of the damaged surface results in the oxidation of all Sn^{2+} defect states and the addition of oxygen or oxygen containing species to the matrix. In this way, the Sn^{4+} stoichiometry (SnO_2) is produced. However, the stoichiometric surface thus produced is still highly amorphous from the alterations induced by ion bombardment. The density of electronic states is surely altered, and the distribution broadened in this disturbed layer. In addition, the EELS spectral shape remains constant with increasing electron primary beam energy, indicating that the amorphous stannic layer is uniform to a depth of at least 10 Å.

The shape of the loss features located between 30 and 40 eV is particularly striking in the spectra of Figure 11. EELS spectra of water plasma treated annealed or "as-deposited" films show a feature in the same region that is almost resolvable into two components (see Figure 5b). The higher energy component is attenuated in the spectra contained in Figure 11. Therefore, the two loss features are not strictly interdependent. These features have been assigned to an O(2s) to conduction band transition and related to the surface oxygen content.[37] If the EELS and XPS data obtained from the water plasma treated, ion-sputtered film are considered collectively, the surface region should be envisioned as largely amorphous layer containing Sn^{4+} cations with a full complement of coordinating oxygen. This implies that the loss component between 35 and 40 eV is sensitive to structural disorder in the SnO_2 lattice and not a direct indicator of surface oxygen concentration. In support of this, it should be noted that the EELS spectra of the Ar^+-bombarded tin oxide film exhibit a similar attenuation of this feature (see Figure 10). Annealing in vacuo of the sputtered surface results in the strengthening of this feature, presumably because of recrystallization of the amorphous layer. If this surface is then water plasma treated, the EELS spectra obtained from it are identical with those of the original surface (see Figure 5, bottom).

Conclusions

The effect of rf water plasma treatment on polycrystalline tin oxide thin films has been investigated by using AR-XPS and EELS. It was found that water plasma treatment of tin oxide films exposed to ambient atmosphere removes surface carbon contamination, oxidizes Sn^{2+} to Sn^{4+} in the surface region, and does not preferentially enrich the surface with hydroxyl groups. Lineshape analysis of the O(1s) peak at different emission angles was used to determine the stoichiometry and thickness of the hydroxylated layer. The thickness of the hydroxylated layer was found to be approximately 10 Å, indicating that an extensive surface "gel layer" does not form on the tin oxide surface as a result of exposure to atmosphere and/or water plasma treatment. EELS and VB-XPS spectra support this assertion by showing that the surface electronic structure is similar to that of the bulk. Experimentally determined surface hydroxyl coverages are a factor of three lower than saturation coverages calculated from crystallographic models.

Vacuum annealing to 600 °C of the water plasma treated tin oxide films resulted in the loss of adsorbed water, dehydroxylation of the surface, and the creation of oxygen vacancies at and below the surface. EELS and VB-XPS spectra obtained from these surfaces indicate that the surface possesses SnO-like character, which is in agreement with other investigations.[24,37] AR-XPS data suggest that a uniform oxygen deficiency exists to a depth of approximately 15 Å.

Water plasma treatment of an oxygen-deficient, SnO-like tin oxide surface prepared by annealing in vacuum regenerates the Sn^{4+} valency and electronic structure of the water plasma treated surface prior to annealing. The oxidation of Sn^{2+} and the filling of oxygen vacancies are simultaneously achieved at room temperature with minimal perturbation to the tin oxide lattice. Water plasma treatment of an oxygen deficient, SnO-like surface created by ion bombardment gives similar results, although the surface retains its structurally disordered state.

We believe that rf water plasma treatment may be a generally applicable method for preparing model, hydroxylated metal oxide surfaces. Future investigations concerned with the interaction of water plasmas with a variety of metal oxide surfaces are warranted to determine if the effects described here for tin oxide surfaces can be extended to other systems and, perhaps, generalized.

Acknowledgment. This research was supported by the National Science Foundation.

Registry No. H_2O, 7732-18-5; SnO_2, 18282-10-5.

Structural and Magnetic Characterization of α- and β-4,4'-(Butadiyne-1,4-diyl)bis(2,2,6,6-tetramethyl-4-hydroxypiperidin-1-oxyl) and Characterization of Its Thermal Degradation Product†

Joel S. Miller,*[1a] Daniel T. Glatzhofer,[1a,b] Rene Laversanne,[1b] Thomas B. Brill,*[1c] Mark D. Timken,[1c] Charles J. O'Connor,*[1d] Jian H. Zhang,[1d] Joseph C. Calabrese,[1a] Arthur J. Epstein,*[1b] Sailesh Chittipeddi,[1b] and Patricia Vaca[1b]

Central Research and Development, E. I. du Pont de Nemours and Co., Inc., Experimental Station 328, Wilmington, Delaware 19880-0328, Department of Physics and Department of Chemistry, The Ohio State University, Columbus, Ohio 43210-1106, Department of Chemistry, University of Delaware, Newark, Delaware 19716, and Department of Chemistry, University of New Orleans, New Orleans, Louisiana 70148

Received October 26, 1989

A new polymorph of 4,4'-(butadiyne-1,4-diyl)bis(2,2,6,6-tetramethyl-4-hydroxypiperidin-1-oxyl), 1, has been prepared. Both phases have been characterized by X-ray diffraction, infrared and Raman spectroscopies, and magnetic susceptibility. The α-phase belongs to the *Pccn* space group [a = 19.049 (4) Å, b = 16.107 (4) Å, and c = 14.113 (3) Å, V = 4330 (3) Å^3, Z = 8, T = −115 °C, R_u = 7.0%, R_w = 8.0%] and the β-phase belongs to the $Pca2_1$ space group [a = 14.265 (1) Å, b = 8.079 (3) Å, and c = 18.865 (2) Å, V = 2174.1 Å^3, Z = 4, T = −100 °C, R_u = 4.8%, R_w = 5.0%]. The molecular structures of both phases are essentially equivalent with the average C≡C, CC—CC, and NO distances of 1.200, 1.385, and 1.288 Å, respectively. The hydrogen bonding OH···ON (or O···O) interactions [i.e., 1.70 (2.834) and 1.72 Å (2.757 Å) for the α-phase and 1.85 (2.804) and 1.84 Å (2.788 Å) for the β-phase] are the only significant intermolecular interactions. Intense ν_{NO} and $\nu_{C\equiv C}$ (Raman) vibrations occur at 1341 and 2236 cm^{-1}, respectively, for both phases. A pleated sheet and helical, hydrogen-bonded solid-state motifs are observed for the α- and β-phases, respectively. On the basis of accepted structural criteria, both solid-state structures should not support single-crystal topochemical polymerization and UV, electron beam, and γ-ray induced polymerization has not been achieved for either phase. Thermal treatment, however, turns the crystals black. Thermogravimetric analysis under nitrogen reveals an explosive decomposition at ~140 °C for both phases. Thermal decomposition monitored by FTIR reveals the loss of the nitroxyl group, destruction of the ring system, and formation of small molecules and a residue more complex than that expected for a simple polymerization. The SQUID magnetic susceptibility of both phases obey the Curie–Weiss expression with θ = ~−1.8 K. The effective moment is ~2.45 μ_B per molecule, which is consistent with two independent $S = {}^1/_2$ spins per molecule. Analysis of the exchange narrowing of the ESR line of α- and β-phases led to an intermonomer exchange of J ~0.165 K (0.115 cm^{-1}). Application of the Weiss molecular field model for the measured $|\theta|$ of ~1.8 K leads to an estimate of ~0.155 K (0.108 cm^{-1}) for the intermonomer exchange J, in very good agreement with the estimate derived from ESR. Upon thermal treatment (~20 h at 80–100 °C) of either phase, a resultant black material forms that exhibit a reduced susceptibility corresponding to <1 μ_B per monomer and nearly zero Curie–Weiss temperature, θ. EPR studies of the thermal degradation products show a complex pattern characteristic of isolated $S = {}^1/_2$ spins interacting with the S = 1 nitrogen nuclear spin and broadened by the dipole interactions with the nearby proton spins. Study of the temperature-dependent EPR of dilute solutions of 1 confirms this analysis and suggests that the majority of the residual spins remaining after heat treatment are monoradicals. The temperature dependence of the intensity of triplet EPR observed for the heat-treated samples suggests the presence of a triplet-exchange interaction of $J_{triplet}$ ~ 10 K. The static and dynamic magnetic data of the thermal degradation products do not provide any evidence for significant 3-D ferromagnetism or even magnetic coupling and indicate the presence of only very weak intradimer ferromagnetic (triplet) coupling.

Introduction

The quest for a molecular-based ferromagnet has culminated with the characterization of decamethylferrocenium tetracyanoethenide, $[Fe^{III}(C_5Me_5)_2]^{\bullet+}$-$[TCNE]^{\bullet-}$, as having bulk ferromagnetic behavior.[2,3] The search for ferromagnetic organic compounds and polymers, however, continues to be of interest.[3-7] Reports of ferromagnetic polymeric materials have been plagued by ill-defined compositions, low yields, lack of characteriza-

† Contribution No. 5024 from E. I. du Pont de Nemours and Company.

(1) (a) E. I. du Pont de Nemours and Co., Inc. (b) The Ohio State University. (c) University of Delaware. (d) University of New Orleans.

(2) Miller, J. S.; Calabrese, J. C.; Bigelow, R. W.; Epstein, A. J.; Zhang, R. W.; Reiff, W. M. *J. Chem. Soc., Commun.* **1986**, 1026–1028. Miller, J. S.; Calabrese, J. C.; Rommelmann, H.; Chittipeddi, S.; Zhang, R. W.; Reiff, W. M.; Epstein, A. J. *J. Am. Chem. Soc.* **1987**, *109*, 769–781. Chittapeddi, S.; Cromack, K.; Miller, J. S.; Epstein, A. J. *Phys. Rev. Lett.* **1987**, *58*, 2695.

0897-4756/90/2802-0060$02.50/0